Reduced number of medial prefrontal cortico-striatal projection neurons in transgenic rat model of Huntington's disease

Stud. med. Arnold J. N Molvær
Faculty of Medicine
University of Oslo

Supervisors: Dr. Trygve B. Leergaard and Dr. Yvette C. van Dongen
Neural Systems and Graphics Computing Laboratory
Institute of Basic Medical Sciences, Department of anatomy
University of Oslo

CONTENTS

FOREWORD

This work was carried out between 2008 and 2010 as a student research project in the Nesys laboratory as a part of Dr. Trygve B. Leergaard's research project: "Structural Neural Network Changes in a Transgenic Rat Model for Huntington's Disease", funded by the Research Council of Norway. The transgenic animals were provided by Professor Stephan von Hörsten (University of Erlangen). The experimental work was conducted by Dr. Yvette C. van Dongen with assistance from research student Arnold Molvær. Eszter Papp assisted with image analysis. Histological processing and analyses were carried out by Molvær. The project was supervised by Drs. van Dongen and Leergaard.

ABSTRACT

Huntington's disease (HD) is hereditary disease, caused by an expanded trinucleotide repeat, which produces cognitive and motor defects, and premature death. Several mouse models have been produced to understand the cause and progression of the disease. However, these models have a short lifespan, and their brains are relatively small with respect to microsurgery. Recently, a homozygote rat model, transgenic for HD, which develops symptoms similar to the late onset form of the disease, has been produced.

The major objective of this study was to evaluate the integrity of the frontal cortico-striatal projection system in a transgenic rat model of HD, by assessing the loss of pyramidal cells in the frontal cortex in this model. We address the hypothesis that corticostriatal projections are reduced in old, symptomatic, transgenic HD rats as found in humans with the disease. We injected the tracer biotinylated dextran amine into the dorsomedial striatum in old transgenic rats (n = 4) and wildtype controls (n = 3), and counted the number of retrogradely labelled neurons in the medial prefrontal cortex. Labelled cells were primarily found in the prelimbic, dorsal anterior cingulated, and medial precentral areas, in correspondence with the known topographical arrangement of frontal corticostriatal afferents (Voorn 2004).

When the number of labelled prefrontal corticostriatal cells per mm^3 of injected tracer in the transgenic HD rat models was compared with the control rats, we observed a found significantly reduced numbers of labelled neurons in the prefrontal cortex ($p = 0.033$). However, given the small sample size, we concluded that further investigations are recommended.

INTRODUCTION

Huntington's disease (HD) is an autosomal-dominant neurogenetic disorder causing motor and cognitive impairments and premature death. The gene responsible for HD encodes a protein called huntingtin (Gutekunst et al., 2002; Craufurd et al. 2002). A mutation within the coding sequence of the gene causes an abnormal expansion of CAG trinucleotide repeats (>28 repeats) in the huntingtin protein. The wildtype huntingtin protein is thought to be associated with various intracellular processes that are essential for normal cell function (Li et al., 2004). The formation of neuronal inclusions and aggregates of mutant huntingtin are key features of the disease. Whether these fragments represent toxic or protective species remains to be clarified (Imarisio et al., 2008).

Another adverse effect, seen in the pathogenesis of HD, is selective neurodegeneration. The process of neuronal degeneration follows a heterogeneous and temporal pattern. The earliest and most prominent neuropathology is found in the basal ganglia (in particular the striatum), followed by many other subcortical and cortical brain regions, including the cerebral cortex (Gutekunst et al., 2002). In the cerebral cortex, topologically selective changes have been identified in symptomatic HD patients (Selemon et al., 2004). This includes regional cortical thinning of the prefrontal cortex (PFC) and is associated with pyramidal cell loss from cortical layers III, V and VI.

The clinical HD symptoms (i.e., motor, cognitive and psychiatric) have traditionally been explained by the dysfunction of the striatum (Bonelli and Hofmann, 2007). However, there is now strong support for an alternative hypothesis on the growing role of the cerebral cortex in the progression of the disease (Lawrence et al., 1998; Cepeda et al., 2003; Rosas et al., 2008). This is further supported by the severe cognitive decline in the middle and late stages the disease.

After the discovery of the gene responsible for HD (The Huntington's Disease Collaborative Research Group, 1993), several transgenic animal models, including a non-human primate model, have been generated (Hickey and Chesselet, 2003; Vonsattel, 2008; Heng et al., 2008; Bugos et al., 2009). Recently, the first transgenic HD rat model has been generated, bearing 51 CAG repeats, which mimics the progressive neurodegenerative changes as observed in adult onset human HD (von Hörsten et al., 2003). Genetically engineered animal models (those of the mice being most extensively studied, while the rat and non-human primate models have only recently been generated) are now frequently used in order to improve our understanding of the pathophysiology of HD. The advantages of the transgenic HD rat model (compared to the mice models) are the longer life span (Ramaswamy, 2007)

and, in particular, the larger size of rats and especially the rat brain, which permits microsurgical techniques and neuroimaging procedures.

AIM

Cortical atrophy and neuropathology are key elements in the progression of HD, and these features are currently understudied. Given the progressive motor and cognitive decline as well as striatal pathology in these transgenic HD rats (von Hörsten et al., 2003; Bauer et al., 2005; Nguyen et al., 2006; Kántor et al., 2006; Cao et al., 2006; Winkler et al., 2006; Temel et al., 2006; Petrasch-Parwez et al., 2007), it is relevant to evaluate the integrity of the underlying neural circuits. The PFC in particular is commonly implicated in cognitive functions and therefore it is likely that this cortical region is involved in the disease process. We hypothesize that cortical projection neurons in the medial PFC (mPFC) are reduced in old transgenic HD rats exhibiting symptoms of HD. To test this hypothesis, we injected the tracer (BDA) biotinylated dextran amine (Veenman et al., 1992; Reiner et al., 2006) into the dorsomedial striatum to retrogradely label the cortico-striatal neurons of the mPFC. The number of retrogradely labelled cortico-striatal neurons in the mPFC was quantified in transgenic HD rats and wildtype littermate controls.

MATERIALS AND METHODS

Animals. Experiments were conducted in five 470±5 days old male homozygous transgenic HD rats (TG group; +/+) and five wild-type littermate control animals (WT group; -/-) provided by our collaborator (Professor Stephan von Hörsten, Friedrich-Alexander University, Erlangen-Nürnberg, Germany). As earlier data (Nguyen et al., 2006) have shown that TG rats develop progressive symptoms of HD from an early age, and striatal atrophy from an age of 12 months, we here consider it likely that the here investigated 16-month-old TG rats have HD-like symptoms and neuropathology (see Fig. 1). As an additional control, experiments were also conducted on two normal 2-month-old male Sprague Dawley rats (SpD group; provided by the Norwegian Institute of Public Health, Oslo, Norway).

All experimental procedures were approved by the local institutional welfare committee of the University of Oslo, in agreement with the European Community regulations on animal wellbeing, and the National Institutes of Health's guidelines for the care and use of laboratory animals

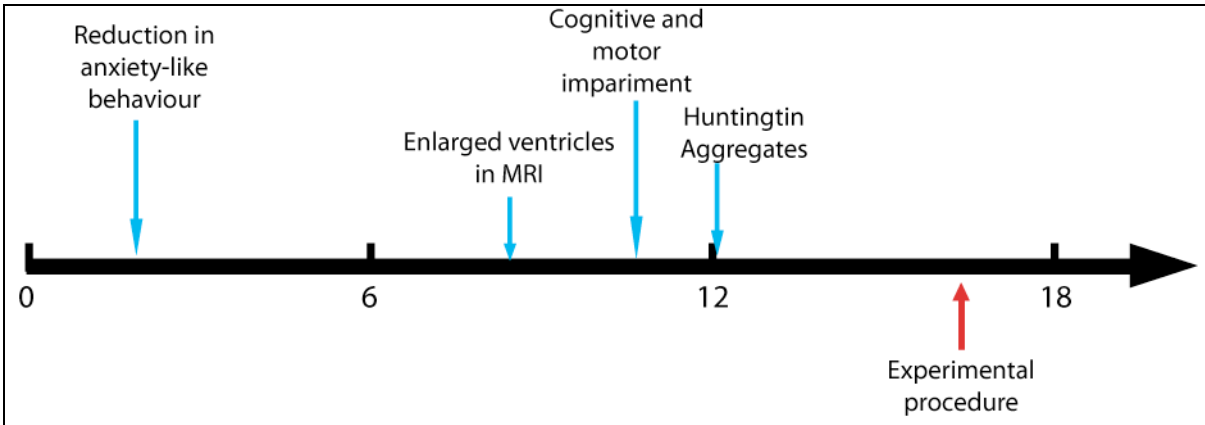

Figure 1. A schematic representation of the rat's lifespan in months, with phenotype changes as described in von Hörsten, 2003.

Animal surgery, tracer injections and histochemistry. Surgical anaesthesia was induced using 5 % isoflurane in a gas chamber. Throughout the surgical procedure anaesthesia was maintained by administration of 2-3 % isoflurane through a muzzle. The rats were placed on a heating pad, and their heads immobilized in a stereotaxic frame using earbars and a toothbar. Vital parameters (heart rate, core body temperature) and level of anaesthesia (pedal reflex) were monitored during the whole procedure. Body temperature was maintained at 37°C using a rectal feedback system. Neutral eye ointment was applied to prevent retinal dehydration.

An incision was made in the scalp, exposing the cranium. The orientation of the skull was adjusted so that the Lambda and Bregma landmarks were horizontally aligned. A small hole was drilled in the cranium at coordinates 1.20 mm posterior and 3.25 mm lateral relative to Bregma. BDA (10% 10kMw BDA in 0.1M sodium phosphate buffer [NaPi] pH 7.4) was iontophorically injected (10 μA, 7s/7s on/off, 30 min) into the dorsomedial striatum (4.5 mm below the surface, at a 25° angle) using a glass micropipette (inner diameter 20μm). Following the injection, the pipette was left in situ for 10 minutes, and then slowly retracted to reduce backflow of the tracer. The skin was sutured and 1 ml saline and Temgesic (0.3mg/ml; 0.1-0.3mg/kg) were injected subcutaneously after the surgery was completed. Nine experiments were successfully conducted, while one animal was euthanized before the procedure was completed.

After a 7 days postoperative period, the animals were re-anesthetized with Nembutal (100 mg/ml; 50mg/kg) intraperitoneally and transcardially perfused with 250-300 ml 9 % saline (at 37°C), followed by a 300 ml 4 % paraformaldehyde (PFA) solution, and finally 250-300 ml of a 10% sucrose solution (at 4°C). All solutions were phosphate buffered and freshly prepared. Following perfusion, the brains were dissected out, and stored in a 30% sucrose solution refrigerated at 4°C until further processing. The lateral surface of the right hemisphere was marked with a shallow razor blade cut along its entire length. The angle of the sectioning of the coronal plane was defined by adjusting the dorsal surface of the brain into the horizontal plane, matching the flat skull position employed in the Paxinos and Watson atlas (2005). Coronal sections (50 μm thick) were cut using a freezing microtome. Each section was stored in separate wells filled with NaPi and 0.1% PFA for long-term storage at 4 °C.

Every second section from the forebrain was stained for BDA using Vectastain's ABC-kit and DAB as a chromogen (enhanced by ammonium-nickel-sulphate), following steps 1-7 in Lanciego and Wouterlood (1994). Sections including the prefrontal cortex were subsequently counterstained with a standard Thionin staining, mounted, dehydrated and coverslipped using Eukitt mounting medium (Van Loenen Instruments, Zaandam, The Netherlands).

Anatomical analysis. The distribution of BDA labelled cells in the left mPFC was mapped in every second section of the mPFC. In each case 24 sections were investigated. The numbers of BDA labelled neurons were recorded in digital section drawings made through a 10x objective using a motorized Zeiss Axioskop2 system running Neurolucida 7

(MicroBrightField Inc., Williston, VT, USA) software. In each drawing the boundaries of the mPFC subregions, the outer contour of the brain and the boundaries of the white matter (external capsule and corpus callosum) were outlined.

The boundaries of the mPFC subregions (i.e., medial orbital (MO), infralimbic (IL), prelimbic (PL), dorsal anterior cingulate (ACd) and medial precentral (PrCm)) were delineated on the basis of cytoarchitectonically-defined criteria (Table 2; Palomera-Gallagher et al., 2004; Vogt et al., 2004; Heidbreder and Groenewegen, 2003; Uylings et al., 2003; Van de Werd and Uylings, 2008). In brief, PL, IL and ACd were located between the Fr2 and MO in mPFC. These boundaries were identified by the relatively thick layer I in this region. PL was distinguished from IL by the presence of a thick layer VI, a thin layer II, and a more distinct layer III. ACd was further distinguished from PL by the double lamination pattern in layer VI, and the homogenous layer III found in ACd. The frontal cortex was delineated on basis of the thin layer I (compared to the ACd, PL and IL), the densely packed pyramidal layers, and a very narrow layer IV, which is present in the previous subregions. Layer III, which is narrower in PrCm as compared to Fr1, was used to distinguish PrCm from Fr1, demarking the superior lateral border of mPFC. The MO was distinguished from the cingulate cortex by its thinner layer I (see also Table 2).

In each subregion, the total number of recorded BDA labelled cells was counted. In order to normalize the number of BDA labelled cells to the size of the injection site, the injection size volumes were measured using an image analysis (Papp and Bjaalie, 2009). To achieve this, digital images of entire coronal sections were acquired with a slide scanner (Mirax Scan, Carl Zeiss MicroImaging GmbH, Jena, Germany). Selected parts of the images covering the BDA injection sites were exported from the Mirax Viewer software at reduced resolution (1:4, uncompressed TIFF format). The exported mages were binarized using ImageJ Autothreshold plug-in (National Institutes of Health, USA: http://rsbweb.nih.gov/ij. The binarization settings used for the injection sites were optimized to include the most densely stained core containing labelled neurons, while excluding the labelled fibres emanating from the injection site. Following binarization all images were filtered using a standard ImageJ medial filter of 1 pixel radius. The number of pixels, representing labelling, was counted, and labelled area was calculated on the basis of the known pixel size of the scanner and the known export resolution ratio. Furthermore, volumes were calculated for each series from area and distance separating the measured sections.

RESULTS

Tracer injection sites

In the 12 experiments conducted, BDA was iontophoretically injected into the striatum. The injection sites were targeted to the dorsomedial striatum 1.2 mm posterior of bregma, at 500 μm distance from the lateral ventricle. Two injection sites (one WT and one TG) involved the overlying white matter and were excluded from the study. The remaining ten injection sites were confined to the dorsomedial striatum (see Fig. 2). Four (out of 10) BDA injections also involved the subventricular zone (see Fig. 2). The injection sites were relatively similar in sizes, however, three (cases WT37, TG80 and TG32) somewhat smaller than the other injections (see Fig. 2; Table 3). In one WT control animal only two retrogradely labelled cells were observed in the prefrontal cortex. This was considered as a failed experiment, which was excluded from the study.

Table 1- List of experimental animals included in the present study

ANIMAL GROUPS	CASE #	GENOTYPE	AGE (days)	WEIGHT (g)
SpD	**TS7**	NA	80	420
	TS9	NA	94	414
WT	**WT36**	-/-	475	510
	WT37	-/-	470	571
	WT58	-/-	474	480
TG	**TG31**	+/+	473	550
	TG32	+/+	469	555
	TG52	+/+	470	520
	TG80	+/+	466	463

Table 2 – Characteristic cytoarchitectonic medial prefrontal cortical areas

AREA	SYNONYMS	CHARACTERISTIC FEATURES
Medial precentral (PrCm)	Fr2, M2	Layer III is narrower than in Fr1*
		Thin but visible layer IV*
Medial orbital (MO)		Layer II has a sharp border upon layers I and III***
Dorsal anterior cingulate (ACd)	Cg1	ACd, like PL and IL, has a thick layer I, compared to other subareas*
		Layer III is rather homogeneous*
		No layer IV (agranular)*
		Layer V has large cells*
		Layer VI is thick*
Prelimbic (PL)	PrL, Cg3	Thick layer I, like ACd and IL*
		Layer III is poorly differentiated* and visible as a bright band between layers II and V***
		No layer IV*
		Layer V is poorly differentiated*
Infralimbic (IL)	IL	Thick layer I, like ACd and PL*
		Layer II is thick**
		Layer III is poorly differentiated**
		No layer IV*
		Layer V is thick**
		Layer VI is very thin **

* Palomera-Gallagher et al., 2004; **Vogt et al., 2004; ***Van de Werd and Uylings, 2008

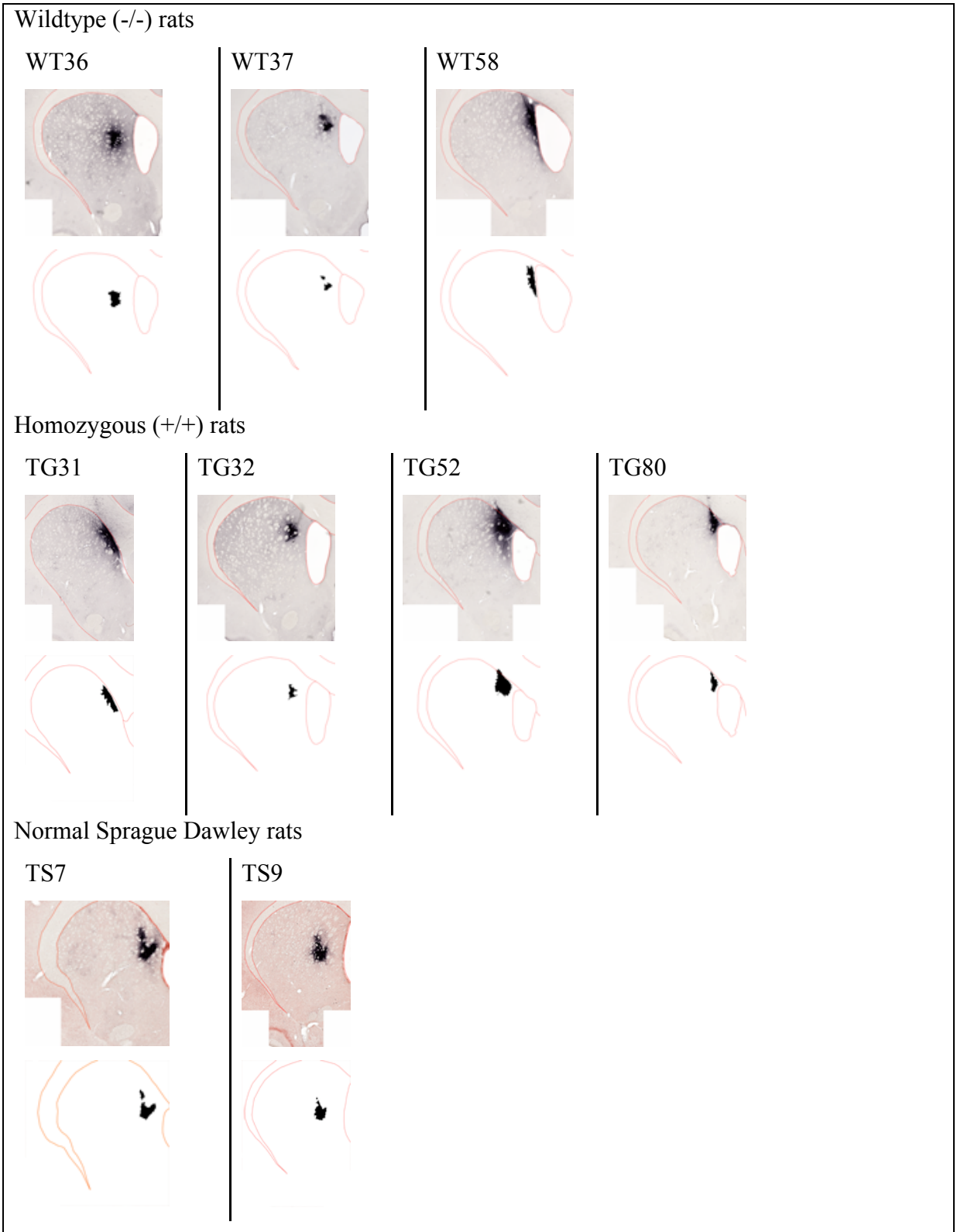

Figure 2. Photomicrographs and corresponding binary image of the injection sites of the tracer biotinylated dextran amine (BDA) in the dorsomedial striatum with the largest diameter.

Table 3 - Injection site volumes

CASE #	TG31	TG32	TG52	TG80	WT36	WT37	WT58	TS7	TS9
Injection site volume	0,145	0,027	0,021	0,018	0,064	0,023	0,191	0,038	0,065

Regional distribution of labelled cells

Histochemistry for BDA revealed labelled cells featuring a typical granular labelling pattern (with or without labelled dendritic fragments; Fig. 3). The labelled cells were distributed throughout the mPFC (Table 4). In the mPFC subregions, the labelled cells were prominent in layer V, and to a lesser extent distributed in layers III and VI (Fig. 4, Table 5). No labelled cells were found in layers I, II and IV. In the medial precentral, dorsal anterior cingulated and PL areas, labelled cells were observed with a higher incidence than in the medial orbital and infralimbic areas (see Fig. 5 and Table 6). There was a qualitatively observed reduction in the number of labelled neurons in the TG rats compared to the WT. These observations had to be confirmed quantitatively, and corrected for their respective injection site sizes.

Quantitative analysis

We counted the number of labelled cells in the mPFC in the TG (n = 4) and wildtype (n = 4) rats, as well as in normal Sprague Dawley rats (n = 2). The labelled cells were found primarily in cortical layers III, V and VI. The WT and SpD rats had a majority of labelled cells in layer V, and, although, this is also true for the transgenic rats, the numbers were greatly reduced (Table 4).

Since the amount of cells labelled are expected to be related to the size of the tracer injection site, we normalized the counted cell numbers to the injection site volume (see Fig. 7 and Table 8). We then compared the number of cells labelled per injected volume of BDA between the three animal groups to test the hypotheses that the numbers of labelled prefrontal cortico-striatal cells reduced in old TG rats. We used an unpaired two-tailed t-test to measure statistical significance.

First, to assess control groups, we compared the number of labelled cells per mm^3 BDA in the wildtype and SpD groups (See Fig. 5 and Table 6). Since there was no significant

difference observed after comparing the numbers in a Student's t-test (p=0.65), we lumped these two groups of animals in a common control group (n=5).

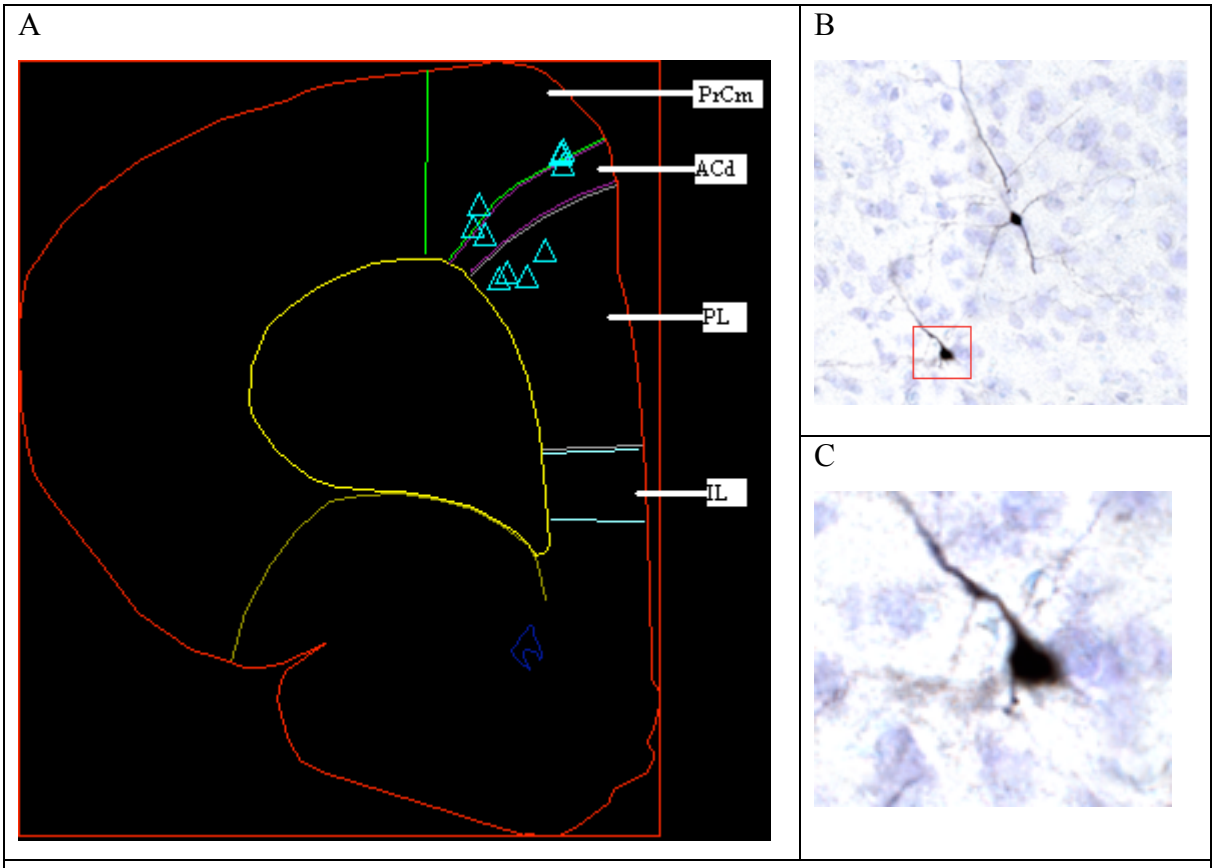

Figure 3. An example of the distribution of retrogradely labelled neurons in the medial prefrontal cortex (mPFC) of a wildtype rat. A) Neurolucida generated digital– recording of a coronal section showing the external brain surface (red), the boundary between cortical grey matter and the underlying white matter (yellow) as well as areal boundaries (white, grey, purple, and green lines), The blue triangles show the distribution of retrogradely labelled neurons in superficial and deep cortical layers. Each triangle represents a single labelled neuron. B is a low power photomicrograph of a thionin stained section, showing BDA labelled neurons in deep cortical layers. C is a magnification of the BDA labelled cell shown in B.

Table 4 – Areal and layer distribution of labelled cells in the medial prefrontal cortex

AREA	Layer	TG31	TG32	TG52	TG80	WT36	WT37	WT58	TS7	TS9	Total
MO	**I**										
	II										
	III										
	IV										
	V	1			1	2		4			8
	VI										
IL	**I**										
	II										
	III										
	IV										
	V							3			3
	VI										
PL	**I**										
	II										
	III **IV**			4		4			7		15
	V	6		35		35	7	34	69	13	199
	VI			1		6	5	3	50	12	77
ACd	**I**										
	II										
	III				1		2	2		1	6
	IV										
	V		3	7		31	48	2	4	15	111
	VI				1	1	5		3	12	22
Fr2	**I**										
	II										
	III	5				1				1	7
	IV										
	V	1	6	4	2	33	14	1		39	100
	VI		5			5	8		1	25	44
Total		13	14	51	5	118	89	49	134	118	592

Figure 4 – Distribution of labelled cells in the medial prefrontal cortical subregions

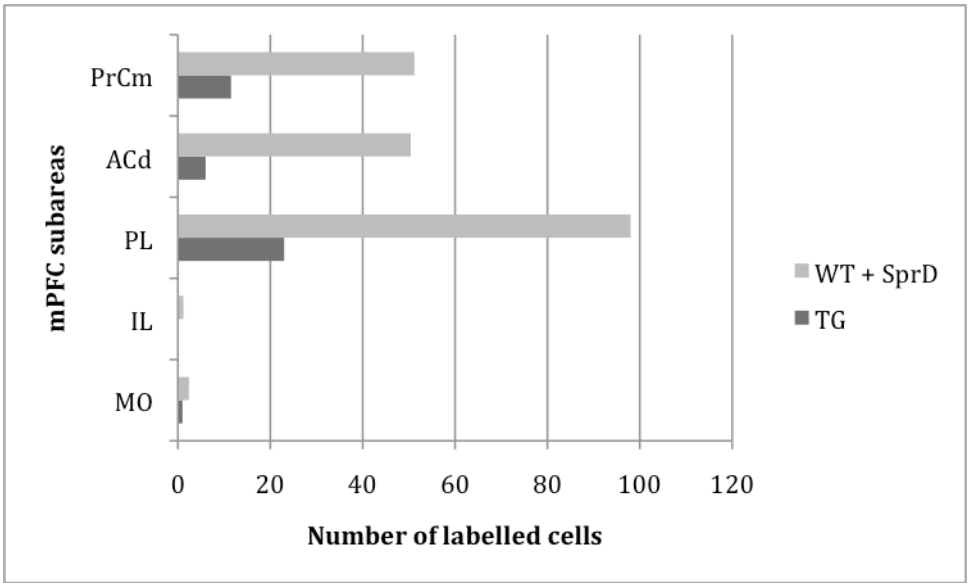

Table 5

AREA	TG31	TG32	TG52	TG80	Sum	Meanx2
MO	1			1	2	1
IL						0
PL	6		40		46	23
ACd		3	7	2	12	6
PrCm	6	11	4	2	23	11,5
Total	13	14	51	5	83	41,5

AREA	WT36	WT37	WT58	TS7	TS9	Sum	Meanx2
MO	2		4			6	2,4
IL			3			3	1,2
PL	45	12	37	126	25	245	98
ACd	32	55	4	7	28	126	50,4
PrCm	39	22	1	1	65	128	51,2
Total	118	89	49	134	118	508	203,2

Since only every second section covering the medial prefrontal cortex was used, the mean is multiplied by two, in order to normalize the values.

Figure 5

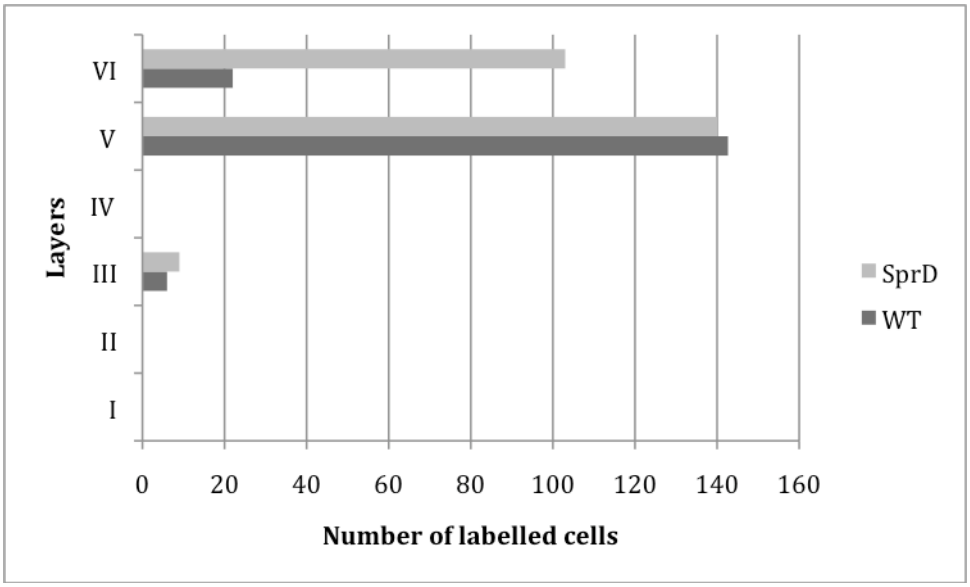

Table 6

Layer	WT36	WT37	WT58	Sum	Meanx2
I					
II					
III	5	2	2	9	6
IV				0	
V	101	69	44	214	142,667
VI	12	18	3	33	22
Total	118	89	49	256	170,667

Layer	TS7	TS9	Sum	Meanx2
I				
II				
III	7	2	9	9
IV			0	0
V	73	67	140	140
VI	54	49	103	103
Total	134	118	252	252

Since only every second section covering the medial prefrontal cortex was used, the mean is multiplied by two in order to normalize the values.

We then compared the total number of labelled cells per volume of injected tracer between the TG rats and the control rats (WT and normal SpD rats). The normalized, mean number of labelled cells was markedly lower in the TG group (41,5) compared to the control groups (203,2). A two-tailed Students t-test showed that this difference was statistically significant (p=0.033) at p < 0,05 (Fig. 6 and Table 7 & Fig. 7 and Table 8).

Figure 6 – Distribution of labelled cells in layers I-VI of the medial prefrontal cortex

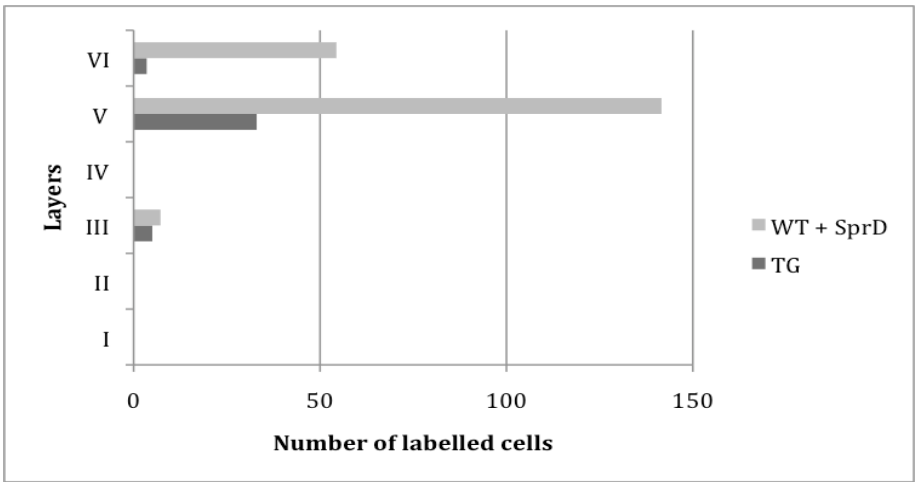

Table 7

Layer	TG31	TG32	TG52	TG80	Sum	Meanx2
I						
II						
III	5		4	1	10	5
IV						
V	8	9	46	3	66	33
VI		5	1	1	7	3,5
Total	13	14	51	5	83	41,5

Layer	WT36	WT37	WT58	TS7	TS9	Sum	Meanx2
I							
II							
III	5	2	2	7	2	18	7,2
IV							
V	101	69	44	73	67	354	141,6
VI	12	18	3	54	49	136	54,4
Total	118	89	49	134	118	508	203,2

Since only every second section covering the medial prefrontal cortex was used, the mean is multiplied by two in order to normalize the values.

Figure 7 – Normalized data: number of labelled cortico-striatal neurons in the medial prefrontal cortex per volume tracer injected

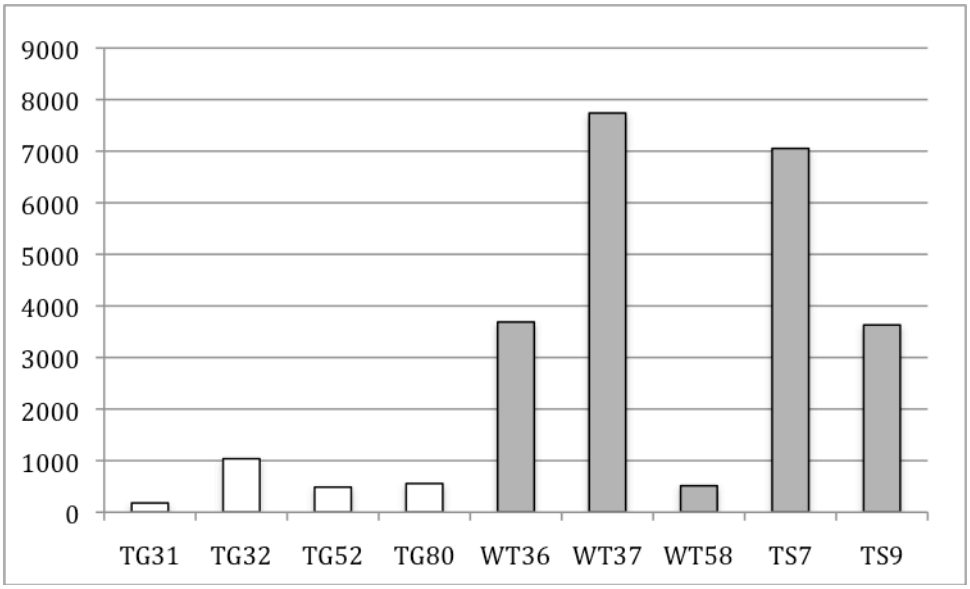

Table 8

CASE #	TG31	TG32	TG52	TG80	WT36	WT37	WT58	TS7	TS9
Inj. site volume (mm^3)	0.145	0.027	0.21	0.018	0.064	0.023	0.191	0.038	0.065
Normalised cell number	26	28	102	10	236	178	98	268	236
Cells per mm^3 tracer	179	1037	485	556	3688	7739	513	7053	3631

The numbers of labelled cells normalized to the size of the injection site (TG rats (white) and the WT + SpD rats (grey))

DISCUSSION

To assess the integrity of the prefrontal cortico-striatal projections in TG rats, we retrogradely traced cortical neurons projecting to the dorsomedial striatum in old TG animals and WT littermates and SpD rats. Quantitative analysis of labelled cells in the medial prefrontal cortex shows a clear tendency towards reduced cortico-striatal projections in the TG animal group, which proved to be statistically significant level.

The tracer BDA (10 kDa) is mainly used as an anterograde tracer, but it is also known to yield retrograde labelling (Reiner and Honig, 2006). It has been reported that the retrograde labelling properties of the tracer can be unpredictable (Vercelli et al., 2000), which could explain the variable numbers of labelled cells in the wildtype rats. The execution of the laboratorial procedures is also prone to both human and reagent errors. To reduce non-specific background staining, hydrogen peroxidase was used. Because there is no automatic way of quantification, human error in counting, overlooking cells, is also a factor to consider. By having two control recounts, with insignificant variations in the numbers, we tried to reduce the possibility of this error.

Despite the statistical significance, the observed results could be extremes within the normal distribution, and that the phenotypical observations merely coincidental. However, there are consistently low numbers of labelled cells observed in the homozygous TG rats when compared to the wildtype rats. To verify if the observed labelling is constant, we need a greater number of specimens to narrow the variation, so as to give a clear answer to the statistical significance of the reduced numbers.

Since the number of specimens used in the present study are few (n = 4), the findings can be interpreted as an indication of what we can expect in future studies. Though there is some variation present, the tendency is clear, suggesting that this study needs more specimens and the use of a pure retrograde tracer to give conclusive evidence.

ACKNOWLEDGEMENTS

Financial support was provided by the Norwegian Research Council (FRIBIO, Leergaard; FUGE2, Bjaalie) and the Institute of Basic Medical Sciences (Leergaard). We thank Jan G. Bjaalie for access to laboratory facilities and infrastructure, Anna T. Bore for expert technical assistance with histological processing, and PhD students Eszter Papp and Izabela Zakiewicz for assistance with injection site volume measurements.

REFERENCES

Bauer A, Zilles K, Matusch A, Holzmann C, Riess O, von Hörsten S (2005). "Regional and subtype selective changes of neurotransmitter receptor density in a rat transgenic for the Huntington's disease mutation." Journal of neurochemistry **94**(3): pp 639-650.

Bonelli RM, Hofmann P (2007). "A systematic review of the treatment studies in Huntington's disease since 1990." Expert opinion on pharmacotherapy **8**(2): pp 141-153.

Bugos O, Bhide M, Zilka N (2009). "Beyond the Rat Models of Human Neurodegenerative Disorders." Cellular and molecular neurobiology.

Cao C, Temel Y, Blokland A, Ozen H, Steinbusch HW, Vlamings R, Nguyen HP, von Hörsten S, Schmitz C, Visser-Vandewalle V (2006). "Progressive deterioration of reaction time performance and choreiform symptoms in a new Huntington's disease transgenic ratmodel." Behavioural brain research **170**(2): pp 257-261.

Cepeda C, Hurst RS, Calvert CR, Hernández-Echeagaray E, Nguyen OK, Jocoy E, Christian LJ, Ariano MA, Levine MS (2003). "Transient and progressive electrophysiological alterations in the cortico-striatal pathway in a mouse model of Huntington's disease." The Journal of Neuroscience **23**(3): pp 961-969.

Craufurd D and Snowden J (2002). Neuropsychological and neuropsychiatric aspects of Huntington's Disease. Gillian Bates, Peter S. Harper, Lesley Jones, Huntington's Disease, Oxford University Press**:** pp 62-94.

Gutekunst C, Norflus F and Hersch S (2002). The neuropathology of Huntington's disease. G Bates, PS Harper and L Jones, Huntington's disease. New York, Oxford University Press**:** pp. 251–275.

Heidbreder CA, Groenewegen HJ (2003). "The medial prefrontal cortex in the rat: evidence for a dorso-ventral distinction based upon functional and anatomical characteristics." Neuroscience and biobehavioral reviews **27**(6): pp 555-579.

Heng MY, Detloff PJ, Albin RL (2008). "Rodent genetic models of Huntington disease." Neurobiology of disease **32**(1): pp 1-9.

Hickey MA, Chesselet MF (2003). "The use of transgenic and knock-in mice to study Huntington's disease." Cytogenetic and genome research **100**(1-4): pp 276-286

Imarisio S, Carmichael J, Korolchuk V, Chen CW, Saiki S, Rose C, Krishna G, Davies JE, Ttofi E, Underwood BR, Rubinsztein DC (2008). "Huntington's disease: from pathology and genetics to potential therapies." The Biochemical journal **412**(2): pp 191-209.

Kántor O, Temel Y, Holzmann C, Raber K, Nguyen HP, Cao C, Türkoglu HO, Rutten BP, Visser-Vandewalle V, Steinbusch HW, Blokland A, Korr H, Riess O, von Hörsten S, Schmitz C (2006). "Selective striatal neuron loss and alterations in behavior correlate with impaired striatal function in Huntington's disease transgenic rats." Neurobiology of disease **22**(3): pp 538-547.

Lawrence AD, Weeks RA, Brooks DJ, Andrews TC, Watkins LH, Harding AE, Robbins TW, Sahakian BJ (1998). "The relationship between striatal dopamine receptor binding and cognitive performance in Huntington's disease." Brain **121**(7): pp 1343-55.

Li SH and Li XJ (2004). "Huntingtin and its role in neuronal degeneration." The Neuroscientist **10**(5): pp 467-475.

Nguyen HP, Kobbe P, Rahne H, Wörpel T, Jäger B, Stephan M, Pabst R, Holzmann C, Riess O, Korr H, Kántor O, Petrasch-Parwez E, Wetzel R, Osmand A and von Hörsten S (2006). "Behavioral abnormalities precede neuropathological markers in rats transgenic for Huntington's disease." Human Molecular Genetics **Vol. 15**(No. 21): 3177–3194.

Palomera-Gallagher N, Zilles K (2004). Isocortex. The Rat Nervous System, 3rd Edition. Elsevier**:** pp. 729-757.

Papp EA, & Bjaalie JG (2009). Automatic detection of labelling patterns in microscopic sections: methods and workflows Frontiers in Neuroinformatics. Conference Abstract: 2nd INCF Congress of Neuroinformatics [doi: 10.3389/conf.neuro.11.2009.08.031].

Petrasch-Parwez E, Nguyen HP, Löbbecke-Schumacher M, Habbes HW, Wieczorek S, Riess O, Andres KH, Dermietzel R, Von Hörsten S (2007). "Cellular and subcellular localization of Huntingtin [corrected] aggregates in the brain of a rat transgenic for Huntington disease." The Journal of comparative neurology **501**(5): pp 716-730.

Ramaswamy S, McBride JL, Kordower JH (2007). "Animal Models of Huntington's Disease." ILAR Journal **Vol. 48 (4)**: pp. 356-373.

Reiner A, Honig MG (2006). Dextran Amines: Versatile Tools for Anterograde and Retrograde Studies of Nervous System Connectivity. Neuroanatomical Tract-Tracing 3, Springer US

Rosas HD, Salat DH, Lee SY, Zaleta AK, Pappu V, Fischl B, Greve D, Hevelone N, Hersch SM (2008). "Cerebral cortex and the clinical expression of Huntington's disease: complexity and heterogeneity." Brain **131**(4): pp 1057-1068

Selemon LD, Rajkowska G and Goldman-Rakic PS (2004). "Evidence for Progression in Frontal Cortical Pathology in Late-Stage Huntington's Disease." The Journal of Comparative Neurology **Vol. 468**(2): pp 190-204.

Temel Y, Cao C, Vlamings R, Blokland A, Ozen H, Steinbusch HW, Michelsen KA, von Hörsten S, Schmitz C, Visser-Vandewalle V (2006). "Motor and cognitive improvement by deep brain stimulation in a transgenic rat model of Huntington's disease." Neuroscience letters **406**(1-2): pp 138-141.

The Huntington's Disease Collaborative Research Group (1993). "A novel gene containing a trinucleotide repeat that is expanded and unstable on Huntington's disease chromosomes." Cell **72**(6): pp 971-983.

Uylings HB, Groenewegen HJ, Kolb B (2003). "Do rats have a prefrontal cortex?" Behavioural brain research **146**(1-2): pp 3-17.

Van De Werd HJ, Uylings HB (2008). "The rat orbital and agranular insular prefrontal cortical areas: a cytoarchitectonic and chemoarchitectonic study." Brain structure & function **212**(5): pp 387-401.

Veenman CL, Reiner A, Honig MG (1992). Biotinylated dextran amine as an anterograde tracer for single- and double-labeling studies. *J. Neurosci. Methods* **41**, pp. 239–254

Vercelli A, Repici M, Garbossa D, Grimaldi A (2000). "Recent techniques for tracing pathways in the central nervous system of developing and adult mammals." Brain research bulletin **51**(1): pp. 11-28.

Vogt BA, Vogt L, Farber BN (2004). Cingulate Cortex and Disease Models. The Rat Nervous System, 3rd Edition**:** pp 705-727.

von Hörsten S, Schmitt I, Nguyen HP, Holzmann C, Schmidt T, Walther T, Bader M, Pabst R, Kobbe P, Krotova J, Stiller D, Kask A, Vaarmann A, Rathke-Hartlieb S, Schulz JB, Grasshoff U, Bauer I, Vieira-Saecker AMM, Paul M, Jones L, Lindenberg KS, Landwehrmeyer B, Bauer A, Li X and Riess O (2003). "Transgenic rat model of Huntington's disease." Human Molecular Genetics **Vol. 12**(No. 6): pp 617–624.

Vonsattel JP, Keller C, Pilar Amaya MD (2008). Neuropathology of Huntington's Disease. Handbook of clinical neurology. **89:** pp 599-618.

Voorn P, Vanderschuren LJMJ, Groenewegen HJ, Robbins TW and Pennartz CMA (2004). "Putting a spin on the dorsal-ventral divide of the striatum." Trends in Neuroscience **Vol. 27**(No. 8): pp. 468-474.

Winkler C, Gil JM, Araújo IM, Riess O, Skripuletz T, von Hörsten S, Petersén A (2006). "Normal sensitivity to excitotoxicity in a transgenic Huntington's disease rat." Brain research bulletin **69**(3): pp 306-310.